Coexistence of bulk superconductivity and charge density wave in Cu_xZrTe_3

Xiangde Zhu,* Hechang Lei, and C. Petrovic
Condensed Matter Physics and Materials Science Department, Brookhaven National Laboratory, Upton, New York 11973, USA

(Dated: June 27, 2011)

We report coexistence of bulk superconductivity and charge density wave (CDW) with superconducting critical temperature T_c = 3.8 K in Cu intercalated quasi-two-dimensional crystals of $ZrTe_3$. The Cu intercalation results in the expansion of the unit cell orthogonal to the Zr-Zr metal chains ($\widehat{b}$ - axis) and partial filling of CDW energy bandgap without obvious shift of CDW transition temperature. $\widehat{b}$ - axis resistivity ρ_b is not related to CDW, and its dominant scattering mechanism for both $ZrTe_3$ and $Cu_{0.05}ZrTe_3$ is the electron - electron Umklapp scattering.

PACS numbers: 71.45.Lr, 74.25.F-, 74.70.-b

Peierls instability results in the periodic modulation of electron density in solids and generates an energy bandgap at the Fermi surface (FS), which leads to insulating behavior in one-dimensional (1D) metal[1]. It can be observed as a charge density wave (CDW) superstructure in many low dimensional materials[2]. Superconductivity (SC), another instability of FS, will also generate a bandgap at FS, which results in a zero resistance. There is a view that SC and CDW orders can only compete with each other. $NbSe_3$, whose structure is composed of infinite $NbSe_6$ trigonal prismatic chains along the monoclinic $\widehat{b}$ - axis, indures two CDW transition with CDW transition temperature (T_{CDW}) = 145 K (T_1) and 59 K (T_2). For example, High pressure continuously suppresses the second CDW transition and induces SC in quasi 1D $NbSe_3$[3]; The suppression of charge order in $Ba_{1-x}K_xBiO_3$ via doping brings out SC with highest $T_c \sim 30$ K[4]; Recently, both Cu intercalation[5] and high pressure [6] in $TiSe_2$ continuously suppress the CDW order, and induce SC with a dome-like phase diagram, which strongly supports the competing view. However, CDW and SC can coexist with each other, like in 2H-$NbSe_2$ with T_{CDW} = 33 K and T_c = 7.2 K[2]. Angle-resolved photoemission spectroscopy (ARPES) results of 2H-$NbSe_2$ show that maximized SC at points in momentum space are directly connected by the CDW ordering vector, demonstrating that charge order can boost SC in electron-phonon coupled system[7], which is in direct contrast to the previous view.

The interplay between CDW and SC is reminiscent of SC in heavy fermion and the cuprate oxide phase diagram when the magnetic order is tuned by pressure (P) or doping to $T \to 0$[8–10]. Superconducting mechanism in such electronic systems is likely to be mediated by the magnetic fluctuations[11, 12]. Similarly, the dome-like structure of $T_c(x)$ and the pairing mechanism in Cu_xTiSe_2 is argued to stem from the type of quantum criticality related to fluctuations in CDW order[13]. Quantum phase transition is proposed to drive CDW order into a quantum nematic phase[14, 15]. On the other hand, the positive slope of the dome could be explained via the shift of the Fermi level caused by Cu intercalation and the negative slope by the enhanced scattering for the high Cu concentration[16]. This is also supported by the evidence for a single gap s-wave order parameter, implying conventional mechanism despite the dome-like evolution of $T_c(x)$[17]. However, a dome-like structure of $T_c(P)$ was also discovered using P as a tuning parameter and suggesting that impurity effects may not be responsible for the dome closure[6].

Chalcogenide superconductors represent a weak coupling side of the smectic order, akin to stripe order in cuprates[14]. There is a mounting evidence that in such systems CDW states transform into Fermi liquid through an intermediate phase[18]. Therefore it is of interest to study the melting of CDW order parameter and possible nematic phases in a superconductor with highly related and tunable two dimensional electronic system.

$ZrTe_3$, as an trichalcogenide (MX_3, where M is the IV-VI transition-metal, and X is S, Se, Te), accommodates the quasi 2D $ZrSe_3$ type structure (shown in Fig. 1 (a))[19, 20], rather than the quasi 1D $NbSe_3$ type structure. The crystallographic $\widehat{b}$ - axis defines the direction of two sets of $ZrTe_6$ trigonal prismatic chains with the shortest Zr-Zr distance. $ZrTe_3$ endures a CDW transition at $T_{CDW} \sim 63$ K with a CDW wave vector $\overrightarrow{q} \equiv (\frac{1}{14}, 0, \frac{1}{3})$[21, 22], and show corresponding hump anomaly on $\widehat{a}$ - axis resistivity (ρ_a) and $\widehat{c}$ - axis resistivity (ρ_c) around T_{CDW}[21]. The FS of $ZrTe_3$ contains one quasi 1D electron like sheet (pocket) of states of $5p$ Te chain origin that is responsible for CDW distortion and pseudogap formation at $T \gg T_{CDW}$[20, 23–25]. $ZrTe_3$ exhibits filamentary SC below 2 K with no diamagnetic response in H = 10 Oe[26]. The CDW and SC in $ZrTe_3$ exhibit rich and so called "competing" interplay under high pressure. With increasing P, the T_{CDW} initially increases below 2 GPa and then decreases up to the vanishing point $T_{CDW} \sim 40$ K at ∼5 GPa[27]; the T_c of filamentary SC decreases and vanish at $P \sim 0.5$ GPa, then a reentrant SC emerges at ∼5 GPa with T_c rising monotonously up to 11 GPa ($T_c \sim 4.5$ K at 11 GPa). Keeping in mind that the FS of $NbSe_3$ mainly origi-

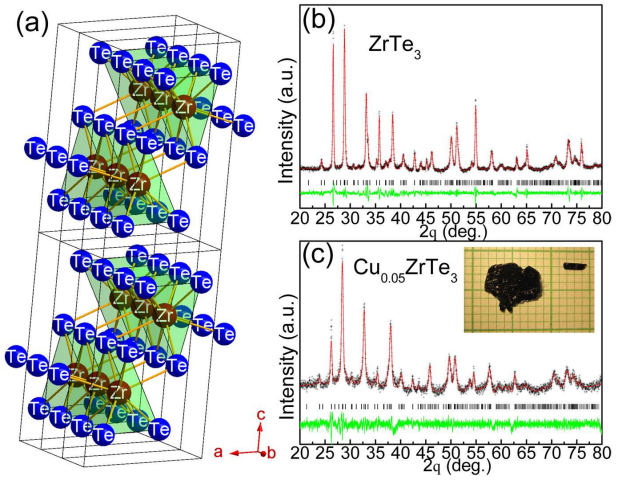

FIG. 1. (a)The crystal structure of $ZrTe_3$ with blue (brown) symbols for Te (Zr) atoms. Comparison of the observed (crosses) and calculated (solid line) powder X ray patterns of $ZrTe_3$ (b) and $Cu_{0.05}ZrTe_3$ (c). The bars (black) correspond to the Bragg reflections and the lowest solid line is the difference between the observed and the calculated patterns.

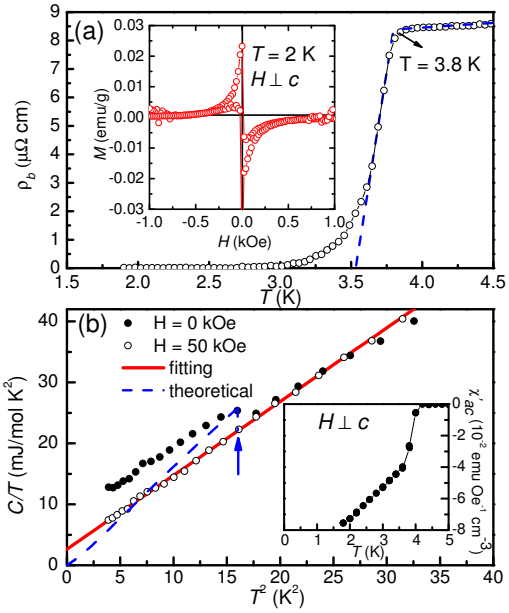

FIG. 2. (a) ρ_b (T) of $Cu_{0.05}ZrTe_3$ near T_c. Inset shows the M-H loop measured at T = 2 K for H⊥c. (b) (C/T) of $Cu_{0.05}ZrTe_3$ as a function of T^2 for H = 0 (solid circles) and H||c = 50 kOe (open circles). Inset shows temperature dependence of χ'_{ac}. See text for details.

nates from the Nb 3d electrons and dome-like structure of $T_c(P)$ in $TiSe_2$, $ZrTe_3$ provides a different opportunity to study the interplay between CDW and SC. Although intercalation attempts have been done in alkali atoms intercalated into $ZrSe_3$[28] and Cu intercalated $ZrTe_3$ via electrochemical method[29], no SC was discovered.

In this letter, we report coexistence of bulk SC and CDW in Cu intercalated $ZrTe_3$. The Cu intercalation results in the expansion of the unit cell orthogonal to $\widehat{b}$ - axis and partial filling of CDW bandgap without obvious shift of T_{CDW}. Anisotropic parameters of the superconducting state are presented. $\widehat{b}$ - axis resistivity (ρ_b) in the normal state is not related to CDW, and its dominant scattering mechanism for both $ZrTe_3$ and $Cu_{0.05}ZrTe_3$ is the electron - electron Umklapp scattering.

Single crystals of $Cu_{0.05}ZrTe_3$ and $ZrTe_3$ with typical size of $1\times3\times0.06$ mm^3 (inset of Fig. 1(c)) elongated along the $\widehat{b}$ - axis were grown via iodine vapor transport method from pure elements sealed in an evacuated quartz tube. After 2 days pre-reacting at 973 K, the furnace gradient was kept between 1023 K and 923 K. Elemental analysis was performed by using energy-dispersive X-ray spectroscopy in an JEOL JSM-6500 scanning electron microscope. The Cu content is determined as the average of the different points on several crystals. Resistivity and magnetization were measured in Quantum Design PPMS-9 and MPMS-XL-5, respectively. The observed (Cu $K\alpha$ radiation of Rigaku Miniflex) and calculated[30] (Rietica software) powder X ray diffraction (XRD) patterns for $ZrTe_3$ and $Cu_{0.05}ZrTe_3$ are shown in Fig. 1 (b) and (c), respectively. Both materials can be indexed to the $ZrTe_3$, indicating that the Cu intercalation does not change the crystal structure. The unit cell refinement yields lattice parameters a = 0.586(3) nm, b = 0.392(7) nm, c = 1.009(5) nm and β= 97.75(1)° for $ZrTe_3$, whereas for $Cu_{0.05}ZrTe_3$ we obtained a = 0.588(2) nm, b = 0.392(8) nm, c = 1.011(1) nm, and β= 97.75(1)°. The Cu intercalation leads to slight expansion of the $\widehat{a}$ and $\widehat{c}$ - axis parameters. It should be noted that Zr - Zr distances along the $\widehat{b}$ - axis chains are unchanged[20].

The onset of SC at T = 3.8 K can be observed in ρ_b, and the magnetization measurements confirm the SC in $Cu_{0.05}ZrTe_3$ (Fig. 2(a)). The shape of the magnetic hysteresis loop of is typical type - 2 inhomogeneous superconductors with some electromagnetic granularity (inset of Fig. 2(a)). This is in agreement with the transition from the temperature dependence of the real part of ac magnetic susceptibility (χ'_{ac}) of $Cu_{0.05}ZrTe_3$ (inset of Fig. 2(b)), and is similar to data in some high T_c cuprates and $SmFeAsO_{0.85}F_{0.15}$[31, 32]. Although the χ'_{ac} does not saturate down to 1.8 K, the large estimated superconducting volume fraction at T = 1.8 K ($4\pi\chi'_{ac} \sim 94\%$) reveals the bulk nature of SC in $Cu_{0.05}ZrTe_3$, as opposed to the pure material[26].

In order to obain the electron-phonon coupling constant λ , specific heat (C) of $Cu_{0.05}ZrTe_3$ was measured. Figure 2(b) depicts the specific heat divided by T (C/T) as a function of T^2 of $Cu_{0.05}ZrTe_3$ in H = 0 kOe and H||c = 50 kOe. Superconducting transition is suppressed in 50 kOe and from its linear fit (solid line depicted in Fig. 2 (b)) $C/T = \gamma + \beta T^2$ (γT is electron contribution, and βT^3 is phonon contribution), we obtain γ= 2.64 ±

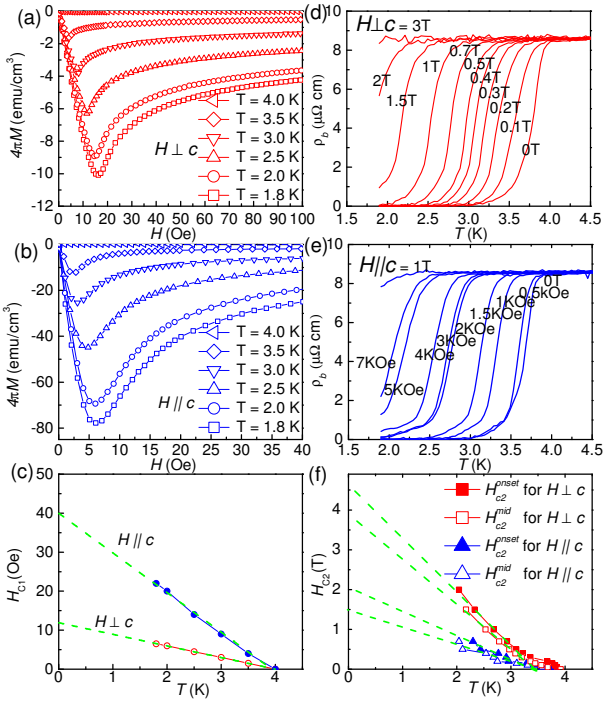

FIG. 3. Field dependence of magnetization of $Cu_{0.05}ZrTe_3$ for H⊥c (a) and H‖c (b). (c) Temperature dependence of H_{c1} for H⊥c and H‖c. The dashed lines are the fitted lines. ρ_b(T) of $Cu_{0.05}ZrTe_3$ for H⊥c (d) and H‖c (e). (f) H_{c2}(T) onset and H_{c2}(T) midpoint (see text) of $Cu_{0.05}ZrTe_3$.

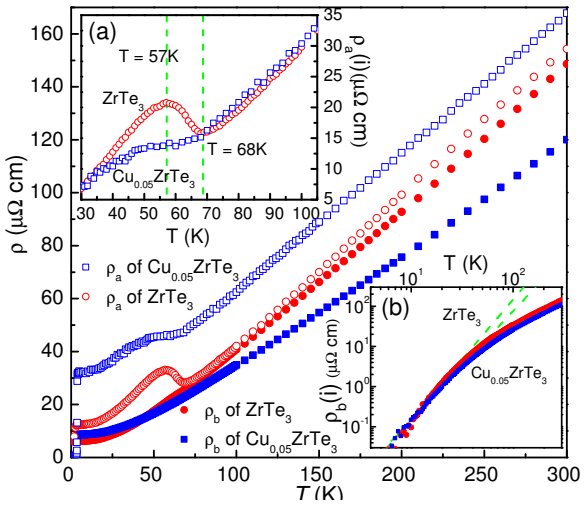

FIG. 4. Temperature dependence of ρ_a and ρ_b for $ZrTe_3$ and $Cu_{0.05}ZrTe_3$. (a) Temperature dependence of $\rho_a(i)$ for $ZrTe_3$ and $Cu_{0.05}ZrTe_3$; the peak (T = 57 K) and the valley (T = 68 K) of CDW anomaly in $ZrTe_3$ are marked with two dashed green lines. (b) Logarithmic plots of temperature dependence for $\rho_b(i)$ with fitting results (dashed green lines) for the Umklapp scattering process (see text).

0.12 mJ/ molK^2 and $\beta = 1.21 \pm 0.01$ mJ/molK^4. A Debye temperature $\Theta_D = 186(1)$ K can be estimated using $\Theta_D = [\frac{1.944\times10^6\times N}{\beta}]^{1/3}$ where N is the number of atoms per formula unit. From the McMillan formula[33]

$$\lambda = \frac{\mu^* \ln(\frac{1.45T_C}{\Theta_D}) - 1.04}{1.04 + \ln(\frac{1.45T_C}{\Theta_D})(1 - 0.62\mu^*)}, \quad (1)$$

we estimate the λ ~0.68 by assuming μ^*= 0.13 for the Coulomb pseudopotential. This is a typical value of an intermediate coupling BCS superconductor. A specific heat jump ($\Delta C/\gamma T_c$) can be observed around T = 4 K (marked by an arrow) confirming bulk SC. The dashed curve depicted in Fig.2(b) is the calculated result of the isotropic BCS gap with $2\Delta/k_BT_c = 3.53$ and $\Delta C/\gamma T_c$=1.43. Although the C data in the superconducting state is not good due to the inhomogeneity, a $\Delta C/\gamma T_c$ larger than 1.43 can be estimated, suggesting the intermediate or strong $e-p$ coupling.

The anisotropic properties of $Cu_{0.05}ZrTe_3$ in the superconducting state are investigated. Figures 3(a) and (b) show field dependence of magnetization of $Cu_{0.05}ZrTe_3$ measured at different temperatures for H⊥c and H‖c. For H‖c, the H_{c1} is obtained using the demagnetization correction[34]. The H_{c1}(T) shows almost linear realtion rather than H_{c1}= H_{c1}(0)[1-(T/T_c)^2] temperature dependence for both field orientation (Fig. 3(c), dashed lines). Thus, we estimate $H_{c1}(0) = -0.693\frac{\partial Hc1}{\partial T}T|_{T=T_c}$ from the Werthamer-Helfand-Hohenberg (WHH) equation[35] and we obtain 8.3(1) Oe (H⊥c) and 27.7(4) Oe (H‖c). Figures 3(d) and (e) show ρ_b(T) of $Cu_{0.05}ZrTe_3$ measured in different fields for H⊥c and H‖c. Figure 3(f) plots the temperature dependence of H_{c2}^{onset} (onset) and H_{c2}^{mid} (midpoint, 50% of ρ in the normal state). $H_{c2}(0)$ are estimated from the linear H_{c2}-T relation with WHH equation. Due to small variance in the in plane resistivity values[21], we assume that coherence lengths are isotropic in the $\hat{a}$ - $\hat{b}$ plane ($\xi_a \sim \xi_b = \xi_{ab}$) and we estimate[36] coherence leghts using $H_{c2}^c(0) = \Phi_0/(2\pi\xi_{ab}^2)$ and $H_{c2}^{ab}(0) = \Phi_0/(2\pi\xi_{ab}\xi_c)$ where Φ_0 is the flux quantum. The Ginzburg - Landau (GL) parameters κ_i and penetration depths are estimated from $H_{c2}^i(0)/H_{c1}^i(0) = 2\kappa_i^2/\ln\kappa_i$ (i = ab, c) and $\kappa_{ab}(0) = \lambda_{ab}(0)/\xi_c(0)$, respectively. Finally, from $H_c(0) = H_{c1}^{ab}(0)/\sqrt{2}\kappa_{ab}(0)$, we estimate the thermodynamic critical field. The anisotropy in obtained superconducting parameters can be approximately estimated from the anisotropic GL relation:

$$\gamma_{anis} = \sqrt{\Gamma} = \frac{H_{c2}^{ab}}{H_{c2}^c} = \frac{\xi_{ab}}{\xi_c} = \frac{\lambda_c}{\lambda_{ab}} = \frac{\kappa_{ab}}{\kappa_c} \sim \frac{H_{c1}^c}{H_{c1}^{ab}} \quad (2)$$

where $\Gamma = \frac{m_c^*}{m_{ab}^*} = \frac{\rho_c}{\rho_{ab}}$ with the effective electron mass m_i^* along the i direction. The obtained mass tensor anisotropy $\Gamma \sim 7$ is comparable with the experimental resistivity ratio ~ 10 of $ZrTe_3$. [21] This points to small anisotropy in the gap function $\Delta(k_F)$.[37] We list the obtained superconducting parameters in Table 1.

The in-plane anisotropic electronic transport proper-

TABLE I. Superconducting State Parameters for $Cu_{0.05}ZrTe_3$.

$Cu_{0.05}ZrTe_3$		$H^i_{c2}(0)$ (kOe)	$H^i_{c1}(0)$ (Oe)	$H_c(0)$ (Oe)	$\kappa_i(0)$	$\xi_i(0)$ (nm)	$\lambda_i(0)$ (nm)
$i = ab$	*onset*	32(4)	8.3(1)	240(30)	93(14)	16(1.2)	605(210)
	mid	27(3)		225(27)	85(11)	18(1.8)	570(184)
$i = c$	*onset*	13(2)	27.7(4)	330(50)	28(5)	6.5(1.3)	1490(420)
	mid	10(2)		295(50)	24(5)	6.7(1.3)	1539(477)

ties in the normal state of $Cu_0.05ZrTe_3$ and $ZrTe_3$ are studied. Fig. 4 shows the temperature dependence of ρ_a and ρ_b for $ZrTe_3$ and Cu_xZrTe_3, which indicates the absolute value of resistivity is quasi 2D for both of them. Since the residual resistivity (ρ_0) is related to the temperature independent defect scattering contribution, resistivity subtracted by ρ_0 (ρ(i) = ρ - ρ_0) can provide information about CDW or scattering mechanism. Compared with $ZrTe_3$ (Fig. 4 (inset,a)), a weaker anomaly below 68 K in ρ_a(i) for $Cu_{0.05}ZrTe_3$ can be observed without a obvious shift. This is in contrast to shift of anomaly in $ZrTe_3$ under high pressure[27] and 1T-$TiSe_2$ by Cu intercalation or under high pressure[5, 6]. Since the resistivity anomaly (shown in Fig. 4 (inset, (a)) comes from of the reduction of DOS at FS due to the CDW bandgap, the weaker anomaly reflects that the CDW bandgap is partially filled via Cu intercalation. Meanwhile, the Cu intercalation has no significant effect on ρ_b(i) (shown in Fig. 4 (inset, b)), even though the absolute values of resistivity are quasi 2D[21]. The scattering along the $\widehat{b}$ - axis in the intercalated and the pure material are not related to the CDW. Linear relation of $\rho_b(i)$ shows that the dominant scattering channel along Zr-Zr metal chains in both materials is electron-electron Umklapp scattering (Fig. 4 (inset, b)), as expected for quasi one dimensional chains[38]. The Umklapp process will result in a $\rho(T) = \rho_0 + AT^n$ (where $2 \leq n \leq 3$) for $k_BT < (0.1 - 0.3)|\delta|$, and a linear relation at high temperature for $k_BT > |\delta|$[38]. The parameter A is a constant and the $|\delta|$ is the typical inter-chain interaction energy. The power law temperature dependence is observed for T < 25 K with $n = 2.98 \pm 0.03$ and $n = 2.70 \pm 0.03$ for $ZrTe_3$ and $Cu_{0.05}ZrTe_3$, respectively (Fig. 4 (inset,b)). The estimated $|\delta|$ range is (100 − 250) K, which is consistent with the observed linear ρ_b(T) above 180 K (Fig.4).

Generally speaking, anisotropic lattice expansion via Cu intercalation is different from the isotropic high pressure in $ZrTe_3$. It reminds us that uniaxial pressure in $NbSe_3$ results in different behavior with isotropic high pressures[39], and that most CDW bearing materials are anisotropic low dimensional system. Thus, the isotropic high pressure provides a combined effect in these materials, rather than a simple way of band widening as expected. It appears that $ZrTe_3$ is an good candidate for the systematic study of the interplay and of CDW and SC, and further spectroscopic measurements would be of interest in order to unfold the details of the phonon mode softening and CDW melting as a function of Cu intercalation. Since SC is induced in another layered tritellurides $TbTe_3$ under high pressure[40], it is worthwhile to search SC by doping or intercalation in the family of CDW bearing layered rare earth tritellurides as well.

In summary, we have shown that Cu intercalation in $ZrTe_3$ results in the expansion of the lattice parameters in the $\widehat{a}$ - $\widehat{c}$ direction (orthogonal to Zr - Zr metal chains) and partial filling of the CDW energy gap. Bulk SC with $T_c = 3.8$ K is discovered in $Cu_{0.05}ZrTe_3$, and its superconducting parameters are given. Along the Zr-Zr metal chains, electrical transport is not related to CDW, and the dominant dominant scattering mechanism is the electron - electron Umklapp scattering.

We thank John Warren for the help with SEM measurements. This work was carried out at BNL, which is operated for the U.S. Department of Energy by Brookhaven Science Associates DE-Ac02-98CH10886.

* present address: High Magnetic Field Laboratory, Chinese Academy of Sciences, Hefei 230031, P. R. China

[1] R. E. Peierls, Ann. Phys. Leipzig **4**, 121 (1930).
[2] G. Gruner, Density Waves in Solids, Addison-Wesley, Reading MA 1994.
[3] P. Monceau, et al., Phys. Rev. Lett. **39**, 161 (1977).
[4] R. J. Cava, et al. Nature **332**, 814 (1988).
[5] E. Morosan, et al., Nature Physics **2**, 544 (2006).
[6] A. F. Kusmartseva, et al., Phys. Rev. Lett. **103**, 236401 (2009).
[7] T. Kiss et al., Nature Physics **3**, 720, (2007).
[8] Qimiao Si and Frank Steglich, Science **329**, 1161 (2010).
[9] P. Gegenwart, et al., Nature Physics**4**, 186 (2008).
[10] S. E. Sebastian, et al.,Proc. Nat. Ac. Sc. **107**, 6175 (2010).
[11] P. Monthoux, et al., Nature **450**, 1177 (2007).
[12] D. J. Scalapino, Science **284**, 1282 (1999).
[13] H. Barath, et al., Phys. Rev. Lett. **100**, 106402 (2008).
[14] K. Sun, et al.,Phys. Rev. B **78**, 085124 (2008).
[15] M. Kim, et al., Advanced Mater. **22**, 1148 (2010).
[16] J. F. Zhao, et al., Phys. Rev. Lett. **99**, 146401 (2007).
[17] S. Y. Li, et al., Phys. Rev. Lett. **99**, 107001 (2007).
[18] S. Hellmann, et al., Phys. Rev. Lett. **105**, 187401 (2010).
[19] S. Furuseth, et al., Acta Chem. Scand., Ser. A **29**, 623 (1975).
[20] K. Stöwe and F. R. Wagner, J. Solid State Chem. **138**, 160 (1998).

[21] S. Takahashi, et al., Solid State Commun. **49**, 1031 (1984).
[22] D. J. Eaglesham, et al., J. Phys. C: Solid State Phys. **17**, L697 (1984).
[23] C. Felser, et al., J. Mater. Chem. **8**, 1787 (1998).
[24] P. Starowicz, et al., J. Alloys and Compounds **442**, 268 (2007).
[25] M. Hoesch, et al., Phys. Rew. B **80**, 075423 (2009).
[26] H. Nakajima, et al., Physica B+C **143**, 240 (1986).
[27] R. Yomo, et al., Phys. Rev. B **71**, 132508 (2005).
[28] K. O. Klepp, et al., Z. Naturforsch., B: Chem. Sci. **57**, 1265 (2002).
[29] W. Finckh, et al., J. Alloys and Compounds **262-263**, 97 (1997).
[30] B. Hunter, Int. Un. of Cryst. Comm. Newsletter **20** (1998).
[31] H. Kupfer, et al., Cryogenics **28**, 650 (1988).
[32] C. Senatore, et al., Phys. Rev. B **78**, 054514 (2008).
[33] W. L. McMillan, Phys. Rev. **167**, 331 (1968).
[34] X. D. Zhu, et al., J. Phys.: Condens. Matter **21**, 145701 (2009).
[35] N. R. Werthamer, et al.,Phys. Rev. **147**, 295 (1966).
[36] J. R. Clem, Physica C **162-164**, 1137 (1989).
[37] P. Miranovic, et al., J. Phys. Soc. Japan **72**, 221 (2003).
[38] A. Oshiyama, et al., J. Phys. Soc. Jpn. **45**, 1136 (1978).
[39] Kh. B. Chashka, et al., Physica B **203** 75 (1994).
[40] J. J. Hamlin, et al., Phys. Rev. Lett. **102**, 177002 (2009).